UR-3490-1480



# Measurement of Adenosine Triphosphate (ATP) Content in Single Red Blood Cells Using the Firefly Bioluminescent Reaction



R.K. Kostuk+, A.G. Muhs*
F.H. Kirkpatrick*, C.W. Gabel≠

A unique optical instrument is described which uses the firefly bioluminscent reaction to measure adenosine triphosphate (ATP) levels in single red blood cells. The method allows chemical content level to be associated with individual cell features. The optical instrument consists of a phase contrast microscope to view cells, a pulsed argon-ion laser to rupture the cell membrane, and a photon counting system to measure the bioluminescent yield. The technique has been calibrated against a standard ATP measurement using bulk analysis methods. The ATP loss mechanism for blood cells in a controlled depletion experiment was also investigated.



+ R.K. Kostuk is with the U.S. Coast Guard, Research and Development Center, Avery Point, Groton, CT 06340

* A.G. Muhs and F.H. Kirkpatrick are with the University of Rochester, Department of Radiation Biology and Biophysics, Rochester, NY 14627

≠ C.W. Gabel is with the University of Rochester, Institute of Optics, Rochester, NY 14627

## DISCLAIMER

INTRODUCTION:

Adenosine Triphosphate (ATP) is the main source of energy for cellular activities. A number of characteristics of cells are directly linked to cellular levels of this compound for normal cell functioning and development. For instance, in the case of red blood cells, it is suspected that their shape and deformability are controlled in part by the cell's ATP level. Maintenance of normal cellular flexibility is necessary for passage through the microcirculation. It is possible that release of blood cells from the bone marrow might also require specific ATP levels.[1,2]

A number of abnormal red cell types are also suspected of having identifying physical characteristics associated with specific ATP levels. Pyruvate kinase (PK) deficiency is characterized by the presence of a greater than normal number of reticulocytes (young blood cells) in the blood plasma, and "young" reticulocytes have a different shape from mature erythrocytes. Another disease, sickle cell anemia, is character-

ized by blood cells with abnormal shapes.

In each of the above cases, identification of cell types in a heterogeous population is possible with conventional microscopy techniques[3] (Fig.1). However, currently available instruments can only measure the ATP content of entire cell populations. Some cell features, i.e. age, are believed to be related to cell density which facilitates discrimination of certain cell features by centrifuging the blood sample and then measuring different density samples with a bulk ATP instrument. However, accurate measurements using any of these techniques require at least $10^6$ cells for each ATP value.[4]

The instrument described here incorporates a phase contrast microscope which allows the operator to select a single cell for ATP content analysis, and thereby associate chemical level with cell features. This important step allows the instrument to be used to obtain knowledge of the relationship between individual cell features and ATP content not previously available. This new information could have a significant

impact in many areas of blood research.

The actual measurement of ATP is performed by rupturing the cell membrane with a laser pulse which allows the released compound to combine with a surrounding bath of luciferin and luciferase. The mixture bioluminesces, and the emitted light is measured with a photon counting system. The prototype device was conceived by Weed and Bessis[5] and implemented by Lajeunie.[6] A number of component modifications and technique changes have been made on the original system which improves its sensitivity and reliability. The evolved instrument and recent ATP measurements are discussed in this article.

INSTRUMENTATION:

The optical instrument is outlined schematically in Fig. 2. The heart of the optical system is the phase contrast microscope, modified to accomplish the following: 1) allow visual recognition of specific cell features, 2) provide a means for focusing the laser pulse onto the blood cell, 3) optimize collection of flux from the bioluminescent reaction and simultane-

ously minimize the effect of noise produced by background emissions in the luciferin-luciferase preparation. A 100X, 1.3N.A. oil immersion objective provides adequate magnification for viewing the 7.5μm diameter cells and identifying their characteristic shapes. The large N.A. of this objective accommodates flux collection over an angle θ, determined by:

$$N.A. = n \sin \theta$$

where θ is half the total flux collection angle. For this case n is about 1.5 for the immersion oil and N.A. is 1.3 which makes $\theta = 60^{\circ}$. The 100 μm diameter object field of the system is determined by a 1.0 cm aperture located near the PMT. This size proves to be a good compromise between a field large enough for locating an interesting cell and small enough to limit the background signal from low level bioluminescence in the luciferin-luciferase enzyme preparation. The condenser of the microscope is another 100X, 1.3 N.A. objective lens. This lens is used to increase the irradiance of the laser pulse and focus it to a region 1 μm in diameter which is

small enough to rupture only one cell.[7]

The Leitz PHACO objectives used in this system have focal lengths of 1.9 mm, working distances of 0.08 mm, and a depth of focus d' [8] given by:

$$d' = d + \frac{250}{M^2} = \lambda \left[ n^2 - (N.A.)^2 \right]^{\frac{1}{2}} / (N.A.) + \frac{250}{M^2}$$

where M is the system magnification, and d is the depth of focus in object space without considering visual accommodation. Substituting the system values M=2000; $\lambda = 5.145 \times 10^{-4}$ mm; n=1.5; and N.A.=1.3 gives the depth of visual focus as d'=3μm. These objectives have a design conjugate image distance of 170 mm. Using the thin lens approximation, the distance between the focal plane and the object ($X_o$) is seen to be: $X_o = \frac{f^2}{X_i} = \frac{(1.9mm)^2}{(170-1.9mm)} = 0.021$ mm. These constraints produce a fairly critical alignment situation. To solve this problem the condenser is mounted on a precision X-Y-Z mount to allow complete spatial positioning.

The laser (Fig. 2) is directed into the condenser with a dichroic mirror at the base of the

microscope which reflects the shorter blue-green wavelengths and transmits longer wavelength light. This allows passage of most of the light emanating from the tungsten source for microscope illumination, and reflects the laser light for focusing onto the blood cell.

The method used for rupturing the cell's membrane evolved from several considerations. First, the system must operate on one cell at a time. Next, if the enzyme surrounding the blood cells is heated above 60°C, the efficiency of the bioluminescent reaction is reduced. Finally hemoglobin has a spectral absorption peak at 514 nm which is also one of the stronger emission lines of the argon-ion laser. With these conditions, it was decided to use a laser pulse with low total energy to minimize heating effects, and high irradiance to effectively rupture the cell membrane. A Quantrad Corp. Model 71B pulsed argon ion laser is used which has a peak multimode, multicolor power of 3 watts delivered in a 40 μsec pulse. As mentioned earlier, the pulse is focused to a 1 μm diameter

spot giving an irradiance of $3.8W/\mu m^2$ and an energy of 120 μjoules.

Light detection of the bioluminescent reaction is accomplished with a Princeton Applied Research 1109/1120 photon counting system with a cooled RCA-C31034A PMT. The GaAs photocathode of this tube has a nearly constant spectral response from 300 nm to 900 nm with an average Q.E. of about 10%. Although the wide spectral response is not the best situation with respect to background noise, it is advantageous in that it covers the relatively broad bioluminescent emission spectrum (500nm to 640nm), and allows for minor shifts in this spectrum without introducing noticeable changes in the count (the emission spectrum is dependent on the pH of the buffering solution)[9]. The background count generated by the preparation and detection system is about 30 counts per second.

The flux collection scheme consists of the 100X, 1.3N.A. objective in the viewing section of the microscope, and a 63mm focal length lens to reduce the beam to a 4 mm diameter spot at

the photocathode (the GaAs photocathode is a 4mm X 12mm rectangle). The objective collects about 20% of the total bioluminescent flux. Combining this factor with the 10% Q.E. of the photocathode gives a maximum collection efficiency of 2%. Since under optimal conditions, one photon is emitted per consumed ATP molecule, the approximately $9 \times 10^7$ ATP molecules in a blood cell should produce an equal number of photons. Theoretically, a count of $1.8 \times 10^6$ is obtainable. Measurement of ATP from normal red blood cells with our system give average cell counts of $10^5$ during a 20 second period. We are within a factor of 20 of the theoretical limit and obtain a signal to noise ratio of over 160 to one.

An electronic timer sequences the measurement cycle. The timer controls the arrival of the laser pulse, opens and closes the PMT shutter, and activates the frequency meter. A 20msec interval between the laser pulse and the signal to open the PMT shutter eliminates the possibility of damage to the photocathode. An additional 120msec delay allows the PMT shutter to

open fully before photon counting begins. The 20 second counting time is set by the PAR 1109 controls. The millisecond duration signals are controlled by two 74123 monostable multivibrators, and the PMT shutter duration by a 555 timer IC. The tungsten source and TV camera shutters are electrically closed when the flip mirror is moved to its vertical position. Vincent Associates Uniblitz type electro-mechanical shutters are used.

PREPARATION TECHNIQUE:

In order to keep a blood cell at the focus of the laser beam, a special preparation holder was designed (Fig. 3). The mount consists of two 0.17mm thick cover slips with the preparation sandwiched between them. The cover slips and preparation are clamped into an aluminum bracket with a restraining O-ring. It was necessary to use the O-ring because the index matching oil adheres to the cover slips and moves them when focusing the objectives. The resulting mount provides an easily handled system for inserting

new preparations and satisfies the optical constraints of the high power objectives.

To prepare a stationary target with a large bioluminescent reaction yield, several problems had to be overcome. Initially, the blood cells were simply mixed with the enzyme. We found that if we used too much of this solution the cells would drift, making them difficult to rupture and causing the reacting solution to move in and out of the microscope's field of view. This significantly influenced the resulting count. If a small quantity of solution was sandwiched between the cover slips, the cells would not be completely surrounded with the enzyme. This caused considerable signal loss and variability in the measurement. To overcome these problems, the technique shown in Fig. 3 was employed. A drop of silicone oil is placed on the lower cover slip acting as a cup for the blood cell and enzyme solution. Cell motion is greatly reduced, and adequate enzyme coverage of the blood cells is provided with this method.

Another problem encountered during early ex-

periments was low photon yield from the bioluminescent reaction. This difficulty was rectified by increasing the amount of luciferin in the premix solution. An optimum yield was obtained with premix concentrations of 0.33 mg/ml of luciferin, 1.3 mg/ml of luciferase, and 0.4 mg/ml of $MgSO_4$ buffered with glycylglycine. The blood cell solution consisted of 0.005ml whole blood and 0.2ml autologous (i.e. from the same donor) plasma. The preparation placed on the cover slip is 0.001ml of a mixture consisting of 0.01ml of premix and 0.003ml of blood cell solutions.

A typical measurement is carried out by first placing the oil on a cover slip, and then injecting blood cell and premix solutions into the oil. This is enclosed with another cover slip, and the combination secured in the aluminum bracket with the O-ring (Fig. 3), and then placed on the microscope stage. The flip mirror is set in its $45^{o}$ position for viewing on the TV monitor. A cell of interest is centered in the field of view with the microscope stage's X-Y positioners. This is also the location at which the

laser beam is brought to focus. The flip mirror is placed in its vertical position which automatically closes the TV camera and tungsten source shutters. The timer is initiated which switches out a laser pulse to rupture the cell, and after a few milliseconds delay opens the PMT shutter and starts the 20 second count period. At the end of this time the PMT shutter closes and the sequence is repeated on another cell. Cell measurement requires about one minute to complete, and the preparation mounting and focusing about five minutes.

EXPERIMENTAL RESULTS:

After optimizing the signal to 0.8-1.0X10$^5$ counts per lysed cell, it was necessary to calibrate the system to relate these counts to the cellular content of ATP molecules. This was accomplished by depleting the ATP content of control cells in a precise manner, measuring the counts at known stages of depletion. Depletion was accomplished by inhibiting the enzymes which produce ATP, while adding other reagents which caused

the ATP to be rapidly consumed. The inhibitor used was iodoacetamide, which specifically and rapidly inhibits the enzyme glyceraldehyde-3-phosphate dehydrogenase[10], and thereby blocks all re-synthesis of ATP. The existing ATP was depleted by the addition of inosine which is phosphorylated by the cell upon entry, and thereby uses up one ATP per inosine. Cells were incubated with these reagents and samples were taken at various times after stopping the reaction by chilling the cells (this reaction is rapid at 37°C and very slow at 4°C).

The major portion of each sample was analysed for ATP content by a commercial "bulk" method (Sigma Technical Bulletin No. 366-UV, a pyruvate kinase coupled assay measured with a conventional UV-visible spectrophotometer) and the remainder of the cells used for the single cell ATP measurements. In order to duplicate the process occurring in the "bulk" instrument, the blood cells on the single cell instrument were measured at random with respect to their individual features. These values produced photon count distributions

similar to that shown in Fig. 4. The means of these distributions were then compared to the "bulk" ATP value at various states of depletion for blood from three different donors and the results are illustrated in Fig. 5. The "r" values are the correlation coefficients fitting data from each donor to a straight line. Although the slopes differ somewhat between donors, the remarkably good correlations with straight lines indicates a one to one relationship between the bulk and single cell methods. This allows us to determine ATP content from photon counts.

The lines do not pass through the origin; either 0.2 mM ATP is prevented from reacting with luciferase, or the pyruvate kinase based "bulk" assay is consistently 0.2 mM too high. The same result was obtained in each of several experiments. This discrepancy is under investigation, but does not detract from the usefulness of the calibration curve.

The frequency distribution of counts during depletion for one experiment is shown in Fig. 6. It is possible to use this distribution to make

inferences about the biochemical mechanism of ATP loss. The kinetics of ATP loss could be either first order, i.e. $\frac{d(ATP)}{dt} = -K(ATP)$, or zero order, $d(ATP)/dt = -K$ where K is the rate constant. In the former case, cells with higher ATP (either content or concentration) should lose ATP faster than cells with less ATP, and in the latter case ATP should be lost at the same rate.

The results for five experiments, similar to that given in Fig. 6, are presented in Table 1. (Fig. 6 is the data for experiment #1 presented in Table 1). A distribution parameter D for cellular ATP content is obtained by calculating the standard error of the mean and dividing this number by the mean number of counts. D is determined for each of five depletion levels. If first order kinetics is occuring D should remain constant since both the count spread and the mean decrease together, while zero order kinetics would yield an increasing D. For each experiment, the value of D increases giving strong evidence that zero order kinetics is the process taking place.

The actual reaction in this system is probably:

1) Inosine + phosphate $\rightleftarrows$ hypoxanthine + ribose-1-phosphate
2) Ribose-1-phosphate $\rightleftarrows$ Ribose-5-Phosphate
3) Ribose-5-phosphate + ATP $\rightleftarrows$ AMP + phosphoribose phrophosphate (PRPP)
4) PRPP + hypoxanthine $\rightleftarrows$ inosinemonophosphate + Pyrophosphate (IMP)
5) AMP + ATP $\rightleftarrows$ 2 ADP or AMP $\rightarrow$ IMP + $NH_3$

There are other reactions occurring, but this should be the major source of ATP loss. Two ATP's are used up per inosine. Each reaction is first order, but inosine is present in large excess. If the ATP-consuming enzyme (PRPP synthetase, reaction 3), has a very strong affinity for ATP, then the reaction can be pseudo-zero order until the ATP concentration is decreased to about ten times above the affinity constant. Hence we can obtain an upper limit ($\leq 2 \times 10^{-5}$M) for the affinity constant

of the enzyme for ATP without having to isolate it. While the present example is somewhat contrived in the sense that we have manipulated the cell's metabolic machinery by using reagents with known effects, it demonstrates that useful information can be derived from the frequency distribution obtained with the single cell apparatus.

CONCLUSIONS:

The single cell instrument is capable of measuring the ATP content of cells which have been visually isolated from a mixed cell population. Typical counts from a normal red blood cell range from 0.8 to 1.0 x $10^5$ which is within a factor of 20 of the theoretical limit. These counts are obtained over a 20 second interval at a signal to noise ratio in excess of 160. The instrument has been calibrated and was used to determine the depletion of ATP loss from single red blood cells. There are several other photon producing systems found in animals which are readily adaptable to this single cell instrument.

One such reaction involves aqueorin, a substance found in certain jellyfish species which reacts with calcium.[11] This element is important in the control of membrane permeability.[12] The single cell instrument and its associated techniques comprise a unique medical research tool which shows promise of providing significant additions to the knowledge of cell processes.

ACKNOWLEDGEMENTS:

This work was supported by NIH program project (HL 18208) and in part by a NIH RCDA (HL 00146) and by an ERDA-DOE contract with the University of Rochester (pub #3490-1480). Appreciation is extended to Frank Kalk for technical assistance, and James Harper, Elaine D'zliao, and the U.S.C.G. R.&D. Ctr. for editing suggestions.

REFERENCES


1. R.I. Weed, P.L. Lacelle, Red Cell Membrane Structure and Functions, ed. G.A. Jamieson and T.J. Greenwalt (J.B. Lippincott Co., Philadelphia, 1969), p. 318-338.
2. R.I. Weed, P.L. Lacelle, and E.W. Merrill, J. Clin. Invest., Vol. 48, No. 5, 795 (May 1969).
3. M. Born and E. Wolf, Principles of Optics (Pergamon, London, 1975), Ch. 8, p. 424.
4. G.A. Kimmich, J. Randles, and J.S. Brand, Analy. Biochem. 69, 187-206 (1975).
5. R.I. Weed, M. Bessis, C.R. Acad. Sc. Paris, t. 278, Série D, 545-547, (21 Jan. 1974).
6. R. Lajeunie, Nouvelle Revue Française d'Hématologie, Tome 14, no. 6, 771-782 (1974).
7. A. Yariv, Introduction to Optical Electronics (Holt, Rinehart, and Winston Inc., 1971), Ch. 3.
8. R. Kingslake, Applied Optics and Optical Engineering Vol. III (Academic Press 1965), p. 157-158.
9. H.H. Seliger, W.D. McElroy, Arch. Biochem.

Biophys. 88, 136-141, (1960).

10. B. Sarkadi, I. Szasz, & G. Gardos, Biochem. & Biophys. Acta 464, 93, (1977). — date

I. Szasz, B. Sarkaki, Y G. Gardos, Heamatologia, 8, 143, (1974).

11. K.T. Izutsu, & S.P. Felton, Clincal Chemistry 18, 77 (1972); J.R. Blinks, F.G. Perendergast, & D.G. Allen, Pharm. Reviews, 28, 1-92, (1976).

12. R.I. Weed, B. Chailley, Erythrocytes, Thrombocytes, Leukocytes (E. Gerlach, K. Moser, E. Deutsch, and W. Wilmanns, eds., Georg Thieme Pub., Stuttgart, 1973), p. 45.

13. Lichtman, M.A., G.V. Marinetti and S.E. Gordesky Nouvelle Revue Francais d'Hemotologie 14 5-24 (1974).

14. M. Nahao in Cellular and Molecular Biology of Erythrocytes ed. H. Yoshikawa and SM.M Rapoport University Park Press (1974).

TABLE 1

Comparison of Distribution Parameters of Fresh and Depleted Cells

A distribution parameter D for cellular ATP content was obtained by calculating the standard error of the mean and dividing this number by the mean number of counts. For samples of similar size, this parameter can distinguish between first order kinetics of ATP loss {d(ATP)/dt=-K(ATP), D does not change} and zero order {d(ATP)/dt=-K, in which case D will increase}. The data indicates the presence of a zero-order process.

DISTRIBUTION PARAMETER D ($\times 10^2$)

| Experiment # | 1 | 2 | 3 | 4 | 5 |
|---|---|---|---|---|---|
| Depletion Step | | | | | |
| 0 | 4.01 | 4.64 | 4.37 | 10.49 | 3.28 |
| 1 | 6.72 | 5.67 | - | 10.36 | 5.63 |
| 2 | 8.56 | 9.76 | 10.34 | - | 7.85 |
| 3 | 10.03 | 11.55 | - | - | - |
| 4 | 15.06 | 14.36 | 17.34 | 14.93 | - |

FIGURE CAPTIONS:

Fig. 1:

Illustration of blood cell shapes (Phase contrast; magnification 800x) panels A through F give typical shape changes of cells in the transition form the normal biconcave shape (A,B) through spiculated forms which are progressively more spherical (C,D,E) to cells which are spherical (F). These are optimal phase contrast images recorded directly on film; television monitor images are not as clear. (Photomicrograph reproduced with permission from Ref. 13).

Fig. 2:

Block diagram of instrumentation used for measuring ATP in single red blood cells. The phase contrast microscope is in the viewing mode when the flip mirror is in the $45^{o}$ position as shown. The X-Y substage positioners move the cell preparation holder to contrally position a cell of interest. The flip mirror is then rotated to its vertical position which electromechanically closes the lamp house and TV monitor shutters. The electronic synchronizer is then triggered which switches out a laser pulse to rupture a blood

cell and then opens the PMT shutter and initiates a 20 second photon counting period.

Fig. 3:

Diagram of preparation holder. An aluminum plate similar in size and shape to a microscope slide has a central opening with an overlapping edge. A cover slip rests on this edge and a drop of silicone fluid is placed on the cover slip. The blood cell and premix solutions are injected into the fluid and sealed in with a second cover slip and retaining O-ring.

Fig. 4:

Histogram showing the relationship between number of cells and photon count for erthrocytes form a normal donor obtained with the single cell instrument when individual cell features were randomized. Approximately 100 cells were ruptured and gave a mean photon count of 90508 $\pm$ 312.

Fig. 5:

Plot showing the relationship between measurements taken on the single cell instrument in a random manner

compared to those made using "bulk" analysis techniques. Cellular ATP was depleted to different levels and then measured with both instruments. The three lines correspond to the results from three different donors. The "r" values are linear correlation coefficients showing the fit of the data to a straight line. Each point for the single cell measurement is the mean of a distribution similar to that given in Fig. 4.

Fig. 6:

Relationship between the percentage of total cells measured in a random fashion on the single cell instrument to the log of the photon count obtained for these cells after various periods of ATP depletion.

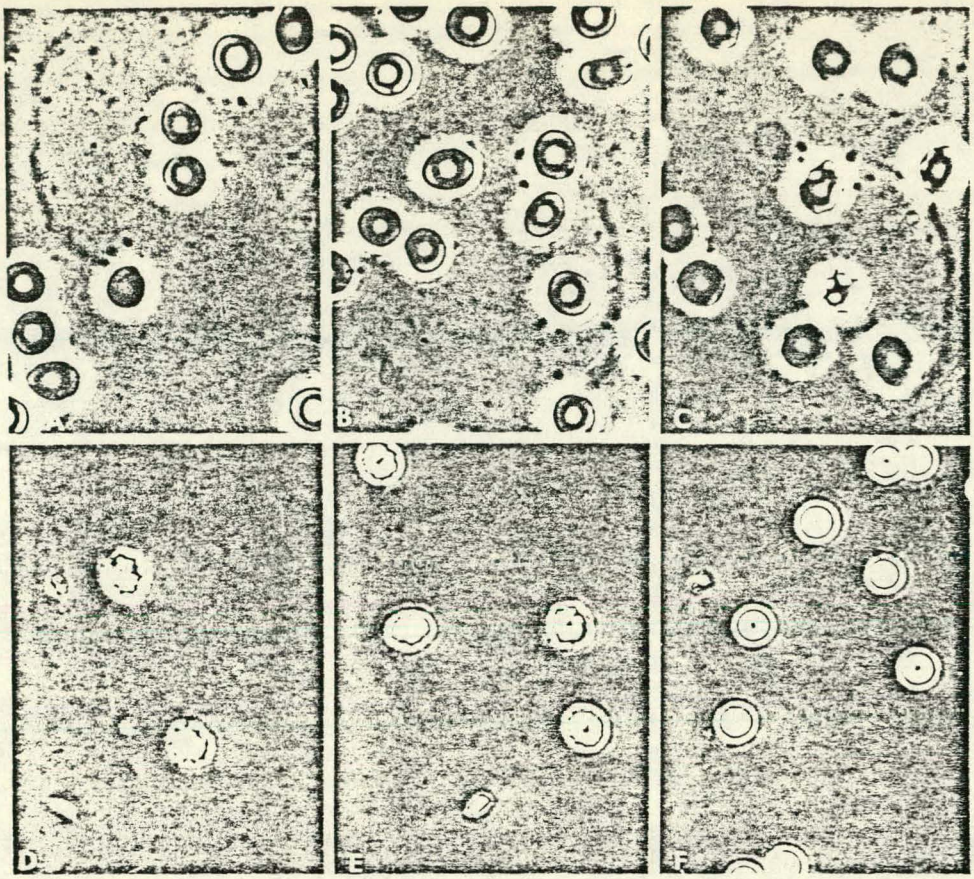

Figure 1.

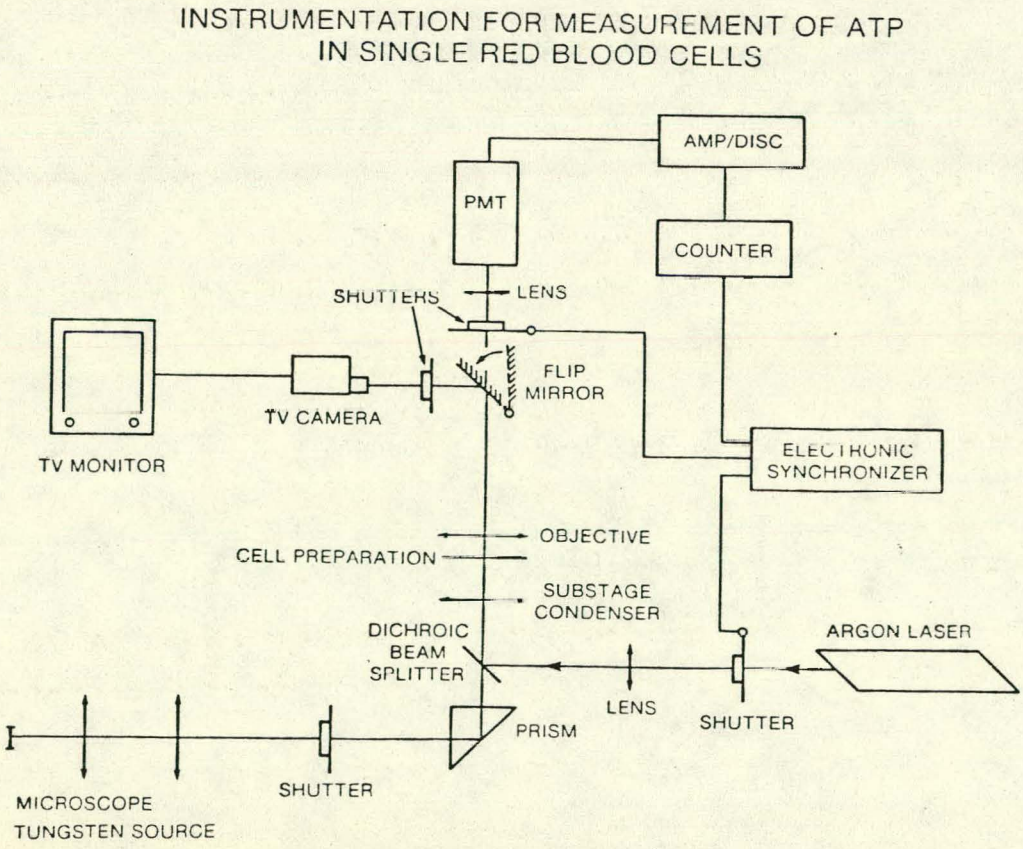


Figure 2.

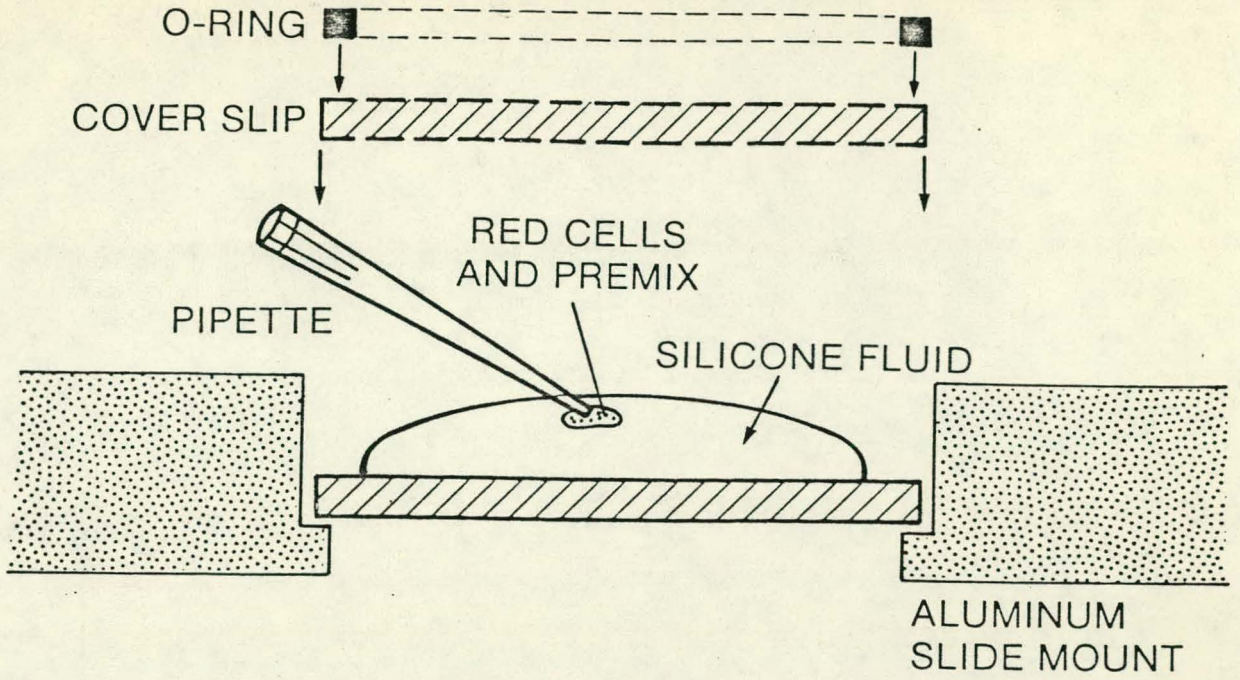


Figure 3

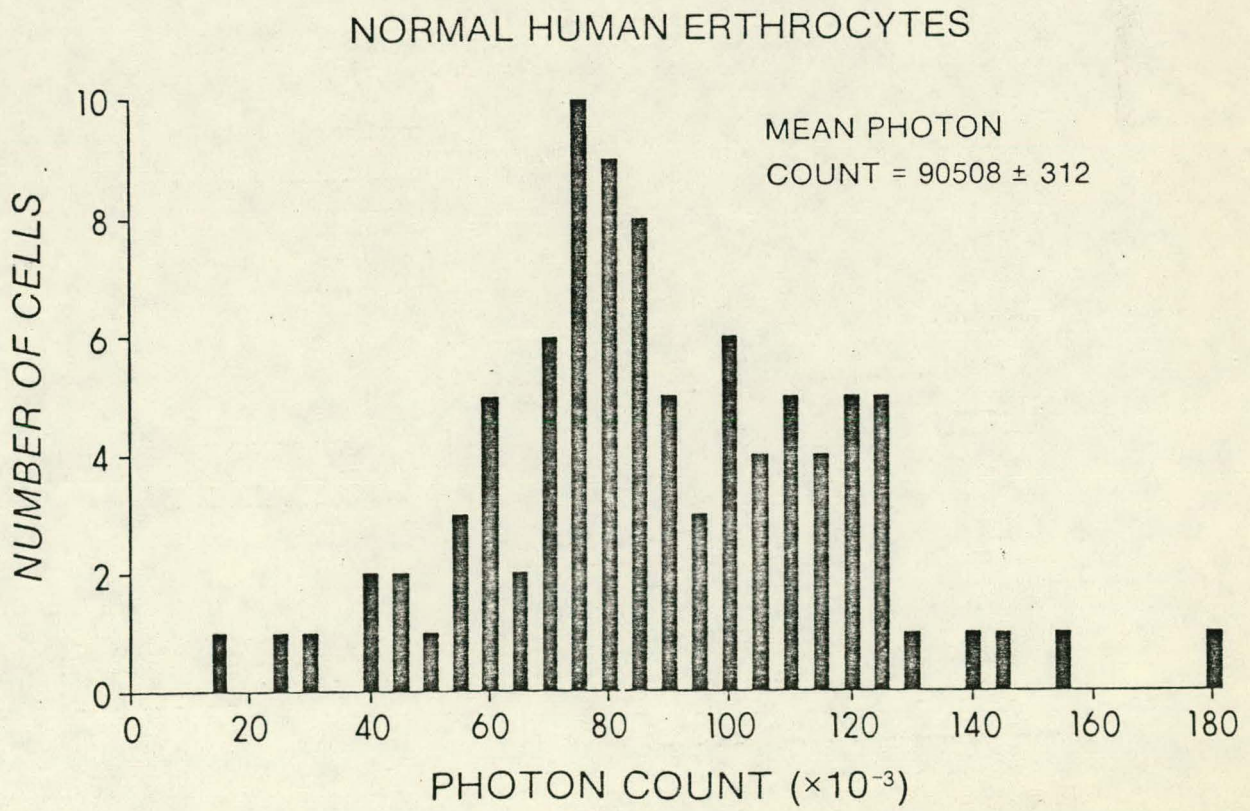


Figure 4

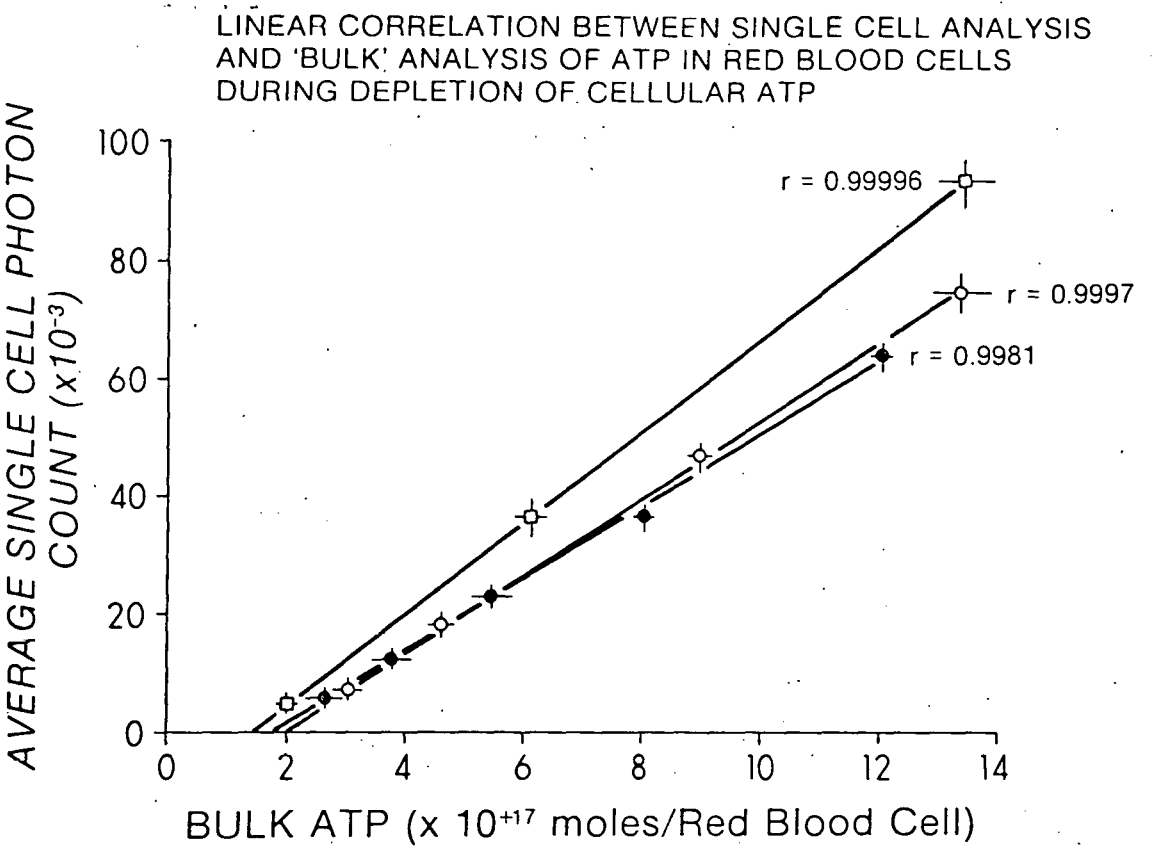


Figure 5

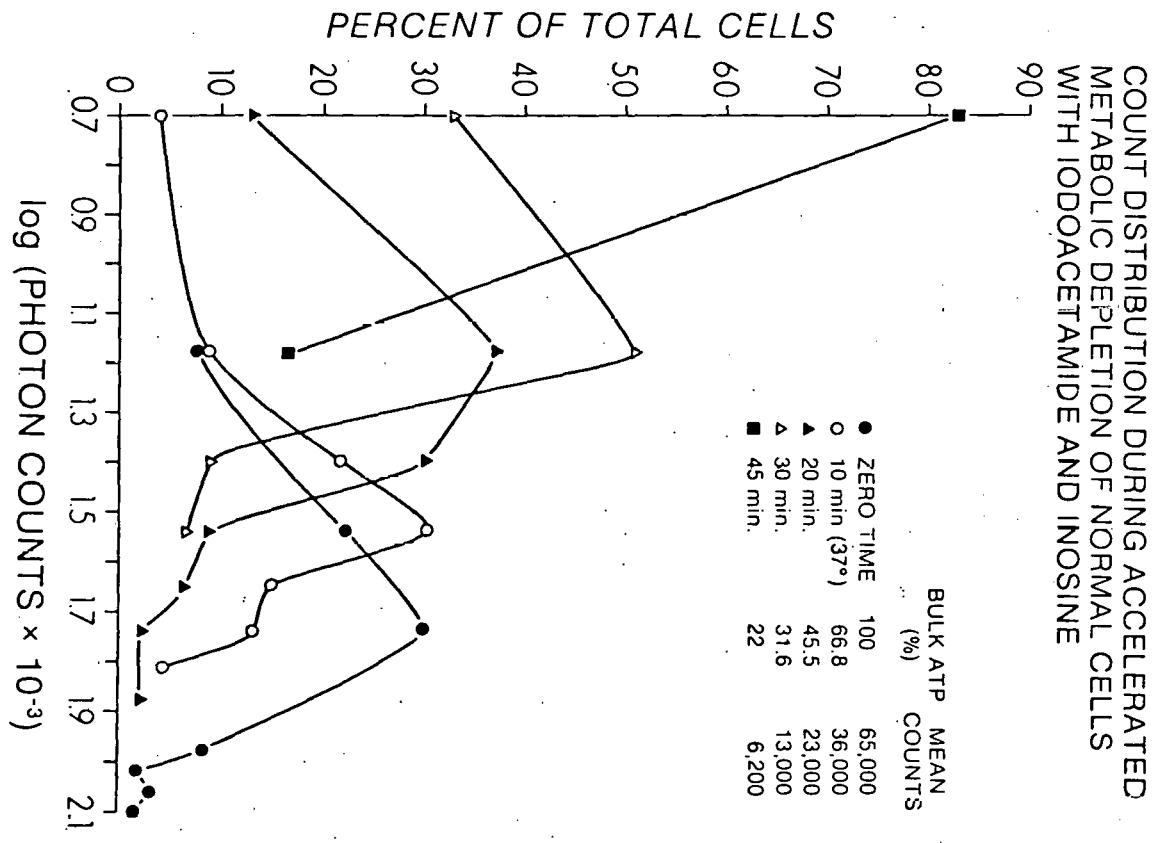


Figure 6